Microwave Packaging of Optoelectronic Components

JOHN SCHLAFER, MEMBER, IEEE, AND ROBERT B. LAUER, MEMBER, IEEE

Abstract—**The design and performance characteristics of single-mode fiber-coupled laser and photodiode packages suitable for use in microwave RF or broad-band transmission systems are discussed. The necessary packaging considerations to achieve laser and photodiode performance to 20 GHz are described. Mechanical, thermal, optical, and microwave details of two laser packages and one photodiode package are given and the optoelectronic characteristics of the packaged units are presented and discussed. It is seen that the intrinsic optoelectronic performance of the components is preserved to at least 20 GHz and that this performance is not affected by package design.**

I. INTRODUCTION

WITH THE demonstration of semiconductor lasers operating in the 15–22 GHz [1]–[5] frequency range and photodetectors capable of operating at frequencies in excess of 35 GHz [6], attention is being directed toward using these components in a variety of analog microwave systems and very high data rate baseband digital systems. Microwave applications include antenna remoting [7], control of phased array radars [8], signal processing applications such as delay lines [9], and subcarrier multiplexed communications systems [10]–[12]. Baseband digital systems have been aimed at the transmission of very high speed data [13] with an important goal being the transport of digital video signals. In order for such systems to be realized, it is necessary to develop packages for the optoelectronic components, the laser and photodetector, which afford microwave environments that do not compromise optoelectronic performance, and that also provide robust mechanical housing. In this paper, two laser packages and a photodetector package are described, and the microwave and optoelectronic performances of these three packages are discussed in detail.

In the second section of the paper the two laser packages are described. The first is a differential laser package [14] which allows the laser to be driven from both ends in a broad-band impedance-matched environment. The second laser package discussed in this section is a modification of the differential, or dual-ended, package. In this case the package is single-ended [15] and the laser is grounded to produce approximately 5 dB increase in the RF coupling efficiency to the laser. The mechanical assembly, the microwave properties, and the optoelectronic characteristics of both of these packages are presented.

In the third section of the paper, considerations relevant to photodetector packaging are given and a package design based on those considerations is described. The performance of this detector package together with a single-ended laser package is described in Section IV.

Manuscript received July 20, 1989; revised October 27, 1989

The authors are with GTE Laboratories Inc., 40 Sylvan Road, Waltham, MA 02254.

IEEE Log Number 8934042.

II. HIGH-FREQUENCY LASER PACKAGES

A. High-Frequency Differential Laser Package

The high-frequency laser package shown schematically in Fig. 1 is designed to allow the laser to be driven by two amplifiers. This produces twice the drive current level possible with a single-ended drive, yet ensures that each amplifier sees a nearly resistive impedance-matched load to maintain amplifier stability. These characteristics make the differential package particularly attractive for very broad bandwidth applications, such as high-speed baseband digital transport, and/or applications where large drive current swings are required.

As shown in Fig. 1, the differential package contains a GTE Laboratories' high-frequency 1.3 μm VPR-BH diode laser [1]–[3], [16] coupled to a single-mode fiber pigtail, an InGaAs edge detector for monitoring the laser's rear facet power, and temperature stabilizing components, all mounted in a hermetically sealed package. The laser and rear facet detector chips are soldered to a diamond heatsink that has been bonded to a copper carrier. A diamond heatsink is used because of its high thermal conductivity and planar mounting surface. These features improve laser reliability by minimizing the temperature rise of the laser's active area. An etched metallization pattern on the diamond forms a 50 Ω microstrip connection to the laser and electrically isolates the laser from the rear facet edge detector. The diamond heatsink and the fiber are each solder-mounted to the copper carrier, which also supports the aligned fiber, a thermistor for temperature sensing, bonding pads, and the microstrip connections to the laser. The fiber inside the package is metallized and attached to a fiber alignment block which is soldered in place in front of the laser. Efficient coupling of the laser to the single-mode fiber is achieved by tapering and lensing the fiber end; typical coupling efficiencies of 20–30% are obtained. Temperature control of the package is accomplished by a thermoelectric heat pump and thermistor which is con-

0018-9480/90/0500-0518$01.00

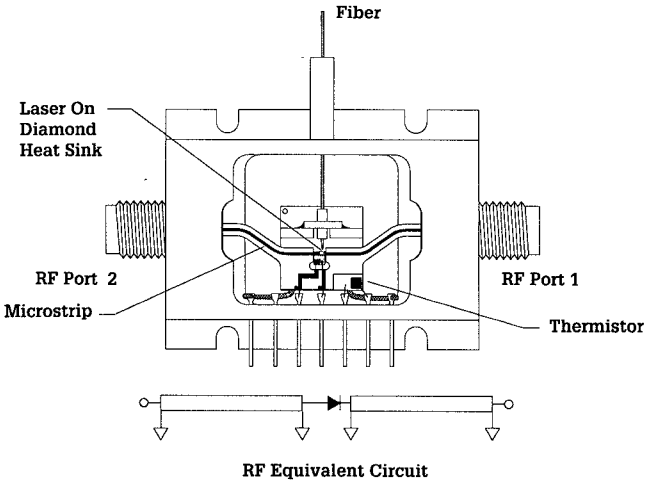

Fig. 1. High-frequency differential laser package allows the series-connected laser to be driven from both ends.

nected in a feedback loop to stabilize the temperature of the laser over a range of -40 to $+70°C$. The transmission line terminating load is placed outside the package where its heat dissipation does not degrade cooling efficiency.

This assembly is housed in a Kovar™ package fitted with low-frequency electrical feedthroughs for bias and control signals, and Wiltron K™ microwave connectors for driving the laser and terminating the transmission line. Stress relief due to differential expansion between the component carrier, package wall, and microstrip is obtained in two ways. The RF feedthrough K-Connectors™ employ a bead assembly having a sliding sleeve on the center conductor to provide a strain-relieved connection to the microstrip. Also, the microstrip lines are formed from flexible Teflon™ substrate material, and accommodate differential expansion between the integral carrier and the package wall. The internal microstrip eliminates excessive inductance associated with long bond wires between the package connectors and laser. Two short bond wires in parallel are used at the microstrip-to-laser and microstrip-to-diamond interfaces to reduce inductance to acceptable levels.

A computer simulation of the differential package was performed to determine the effects of package parasitics on the package equivalent circuit. The equivalent circuit used for the simulation is shown in Fig. 2. The transfer function calculated using SPICE from the input to the laser's light generating port, R_2, shows a passband ripple of ± 0.25 dB for the package, without regard to optical frequency response of the laser. A sensitivity analysis determined that bond wire inductance dominates frequency response. Short parallel bond wires are essential to achieving this low ripple performance. Ripple is also affected by transmission line impedances. A 10% variation increases ripple to ± 1 dB. Based on the SPICE simulations, the laser's frequency response is expected to dominate performance of the differential package to 20 GHz.

Frequency-response measurements using a Hewlett-Packard 8510 network analyzer, displayed in Fig. 3, reflect the dominance of the laser's optical frequency response. The bias current dependence of the resonance peak frequency and 3 dB bandwidth are characteristic of the laser structure [1]–[3]. For this particular laser, a 3 dB bandwidth of 15 GHz is reached at 100 mA drive current, increasing to approximately 18 GHz at 160 mA. The 0.75 dB peak-to-peak ripple in the region below 8 GHz does not appear in unpackaged lasers, and is attributed to this package configuration. The ripple is consistent with that predicted by the SPICE simulation.

A desirable value for return loss in typical microwave applications is 10 dB or greater, corresponding to a voltage standing wave ratio (*VSWR*) of about 2. Return loss was measured on two packages, one containing the same laser used in the frequency response test and the other with bond wire shorts in place of the laser. It was found that the return loss is not materially affected by laser impedance, and a return loss of 10 dB or greater is achieved over the entire band, as seen in Fig. 4. A substantial portion of this reflection appears to be associated with parasitics in the RF feedthroughs.

B. High-Frequency Single-Ended Laser Package

The differential or dual-ended laser package just discussed has its principal strength in the low input reflection coefficient it produces for baseband operation to 20 GHz, but is inefficient in coupling microwave energy into the laser. Improved coupling efficiency can be obtained by driving a grounded laser directly from a 50 Ω transmission line. In this configuration the low-impedance laser is not matched to 50 Ω and produces a large reflection which must be absorbed by the drive circuit. The advantage of this configuration is that the current through the laser is almost twice as large as for wide-band impedance matching using a resistor in series with the laser. The laser current can be determined from $I_L = 2(P_i Z_0)^{0.5}(Z_0 + Z_L)^{-1}$, where P_i is the incident power, Z_0 the characteristic impedance, and Z_L the load impedance. If $Z_L = 3$ Ω is the laser resistance, and $Z_0 = 50$ Ω, the laser current will be 1.9 times greater than if Z_L were matched to 50 Ω by adding 47 Ω in series with the laser. For applications requiring bandwidths of an octave or less, the reflections produced in this unmatched configuration can be absorbed, if necessary, using an isolator between the laser and the drive electronics.

A laser package employing this single-ended unmatched circuit has been implemented as a modification of the differential package described above. The external package is similar to that shown in Fig. 1, except that one output connector is eliminated. A detailed view of the carrier platform is shown in Fig. 5. To this carrier is attached the laser, which is mounted on a diamond heatsink, an optical fiber, a thermistor, a photodiode for monitoring the laser rear facet emission, and a bias insertion inductance. The carrier rests on a thermoelectric heat pump for regulating laser temperature. A flexible microstrip connects the laser to the coaxial feedthrough in the package wall to allow for differential thermal expansion between the thermoelectric cooler mounted carrier and the package wall.

Bias is applied to the laser through an inductor which is formed by using a wire bonder to wind turns of wire on a

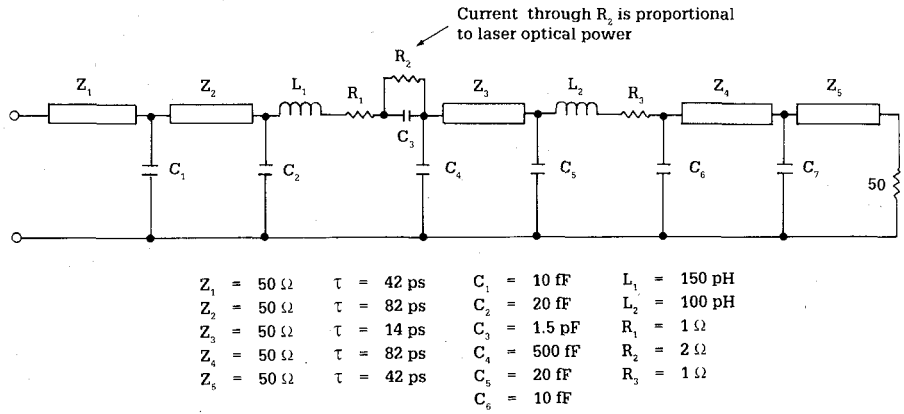

Fig. 2. Equivalent circuit model of differential laser package.

R_2, C_3: Equivalent circuit of laser. Current through R_2 is proportional to optical power.
Z_1, Z_5: Lossless transmission line model of microwave connectors.
Z_2, Z_4: Lossless transmission line model of internal microstrip.
Z_3: Lossless transmission line of microstrip pattern on diamond submount.
L_1, L_2: Bond wire inductances to laser and diamond, respectively.
C_1, C_7: Parasitic capacitance at microwave connector-to-microstrip interface.
C_2, C_6: Parasitic capacitance at microstrip-to-bond-wire interface.
C_5: Parasitic capacitance at diamond-to-bond-wire interface.
C_4: Stray capacitance from p-surface of laser to backside of diamond.
R_1, R_3: Lumped values of bond wire and contact resistances.

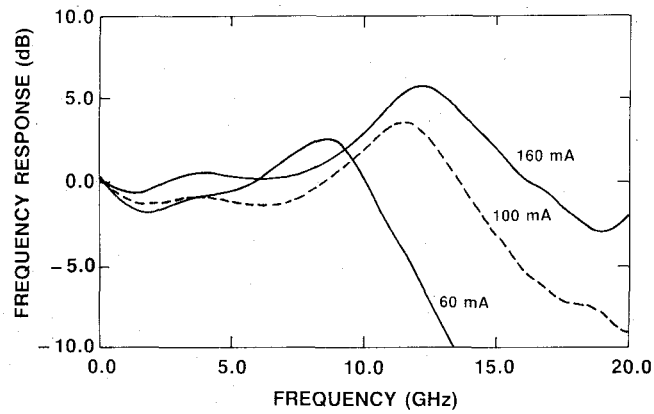

Fig. 3. Normalized frequency response of the differential laser package of Fig. 1, measured with a wide-bandwidth photodetector.

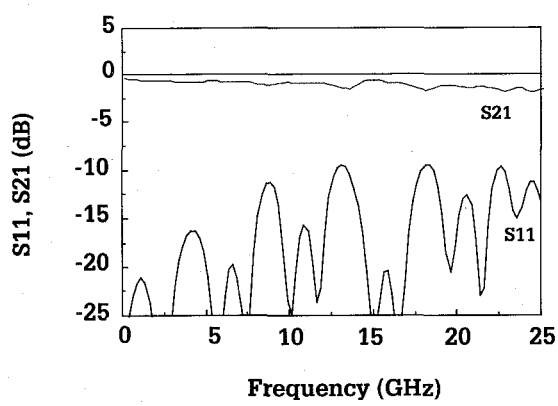

Fig. 4. Electrical transmission and reflection scattering parameters for the differential laser package of Fig. 1.

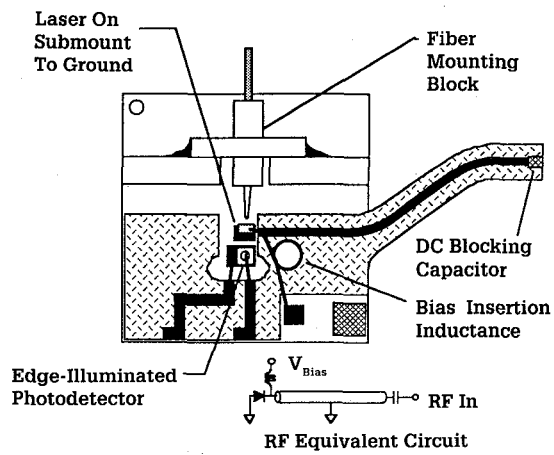

Fig. 5. Detailed view of the carrier assembly for a single-ended laser package.

post placed adjacent to the laser. The inductor is attached to the low-impedance point at the laser end of the microstrip trace. A dc blocking capacitor is located at the microstrip-to-coax transition. The bias network introduces a low-frequency cutoff of about 100 MHz in the RF connections to the laser.

The swept frequency response of the single-ended laser package is similar to that of the differential laser package, and is dominated by the high-frequency characteristics of the laser. The overall performance of the single-ended package will be discussed later in a subsystem context which includes the photodetector package to be described below.

III. High-Frequency Photodiode Package

Packaging of wide-bandwidth photodiodes can be simpler than for lasers, since there is no requirement for temperature control or optical power monitors, and fiber

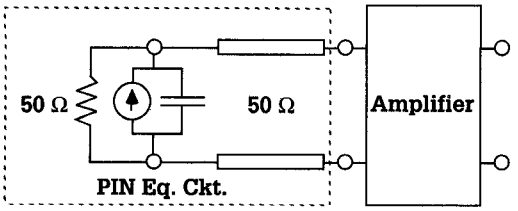

Fig. 6. Schematic of a back-matched photodetector package.

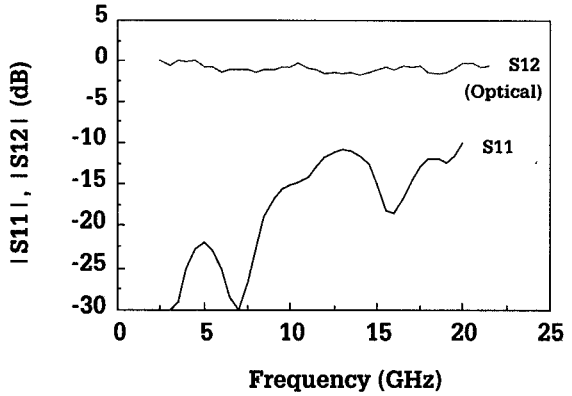

Fig. 7. Electrical response to optical modulation ($|S_{12}|$), and input reflection coefficient ($|S_{11}|$) of matched photodetector package.

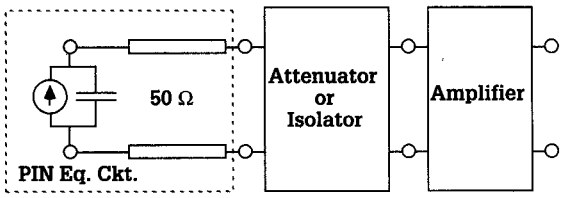

Fig. 8. Schematic of unterminated photodetector package with an optional attenuator or isolator to reduce the effects of reflections.

alignment tolerances are in general relaxed, although the microwave considerations remain stringent. If the output impedance of the photodiode package is required to be 50 Ω over a very broad band, the configuration shown in Fig. 6 may be used. With this connection the available signal power is reduced by 6 dB, since only half of the photocurrent flows toward the output port while the other half is dissipated in the internal matching resistor. This loss may be acceptable if the noise floor of the system is set by the laser relative intensity noise rather than noise in the receiver [17]. The frequency response [18] and S_{11} characteristics of a photodiode packaged with this matching circuit are shown in Fig. 7.

In the most elementary electrical configuration, the photodiode chip is connected directly to the end of a transmission line, as in Fig. 8. This circuit couples all of the signal power into the output port, but in this configuration the impedance of the photodiode does not present a matched load to the succeeding stage. Reflections introduced when operating the photodiode with an amplifier having a significant input reflection coefficient may degrade the flatness of the frequency response characteristic or lead to amplifier instabilities. In applications covering an octave or less

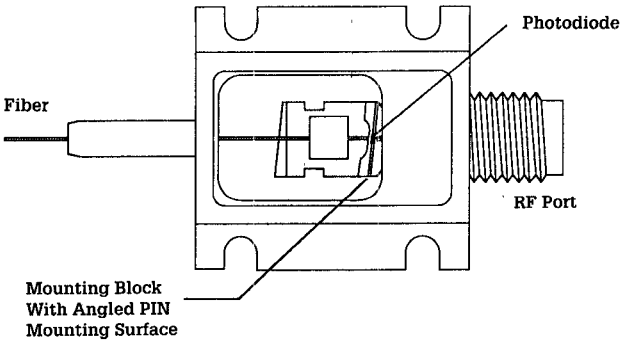

Fig. 9. A fiber-coupled photodetector package which uses the unmatched configuration of Fig. 8 incorporates an angled photodiode mount and fiber end face to increase optical return loss.

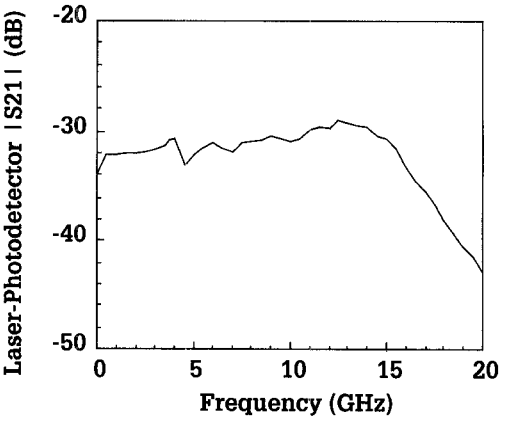

Fig. 10. Magnitude of the transfer function for a fiber-coupled laser-photodetector pair, each mounted in the non-impedance-matched configuration.

bandwidth, an isolator can reduce the effects of this impedance mismatch.

A fiber-coupled package geometry which implements this latter circuit is shown in Fig. 9. A substrate-illuminated mesa-geometry InGaAs p-i-n photodiode chip [19] is mounted perpendicular to the axis of the coaxial feedthrough and connected to it with a short bond wire. Fiber optical access to the chip substrate is through a hole in the mount. To minimize optical reflections the photodiode is tilted 6° with respect to the fiber optical axis and the fiber end is cleaved at 6°. The packaged photodiode frequency response has a 3 dB bandwidth of 22 GHz, a fiber-coupled responsivity of 0.5 A/W at $\lambda = 1.3$ μm, and an optical return loss > 40 dB.

IV. Subsystem Performance

The magnitude of the small-signal transfer function of the single-ended packaged laser and photodiode modules when coupled through a short length of fiber is -32 dB at 1 GHz and rises 3 dB at 13 GHz, the peak of the laser's resonance (Fig. 10). The bandwidth of the system exceeds 16 GHz and is dominated by the laser's frequency response. A ± 1 dB ripple at 4 GHz is caused by reflections in the package between the laser and the microstrip-to-coax transition. The low-frequency 3 dB bandwidth of 0.1 GHz is set by the dc blocking capacitor. The system throughput is determined by such factors as microwave power cou-

pling to the laser, laser differential quantum efficiency, fiber coupling efficiency, and photodiode responsivity [20].

Laser relative intensity noise (*RIN*) was measured with the laser and photodiode coupled through 1.5 km of single-mode fiber using low-reflection splices. With 2.7 mW incident on the photodiode, the maximum *RIN* is -140 dB/Hz at the laser's self-resonance and is less than -145 dB/Hz below 6 GHz. These values are identical to those obtained for the same nonfiber coupled device. If reflections from connectors, splices, or the photodiode package are not suppressed, the *RIN* can increase by as much as 20 dB. For example, if a perpendicular cleave is used on the fiber at the photodiode, optical return loss is reduced to 14 dB, and *RIN* values increase at resonance to approximately -120 dB/Hz.

V. Summary

Two laser packages and one photodiode package capable of excellent performance to frequencies of at least 20 GHz have been described. One of the laser packages, the differential package, allows the laser to be driven by large current swings in a nearly resistively impedance-matched environment, making this package well suited for very high speed baseband digital applications. The second laser package, which is single-ended, is best adapted to narrower ($\sim$1 octave) band microwave applications where the transfer of RF power is the primary consideration. The photodiode package is designed so that noise degrading optical reflections are a minimum, while high responsivity and broad bandwidth performance are maintained.

Acknowledgment

The authors would like to thank P. Baum and M. Teare for performing the SPICE simulation of the differential package. They also wish to acknowledge the expert package assembly performed by R. Sargent and R. Morrison and to thank L. Ulbricht for many helpful conversations.

References

[1] C. B. Su *et al.*, "15 GHz direct modulation bandwidth of vapor-phase regrown 1.3 μm InGaAsP buried-heterostructure lasers under cw operation at room temperature," *Electron. Lett.*, vol. 21, pp. 577–599, 1985.

[2] R. Olshansky, V. Lanzisera, C. B. Su, W. Powazinik, and R. B. Lauer, "Frequency response of an InGaAsP vapor phase regrown buried heterostructure laser with 18 GHz bandwidth," *Appl. Phys. Lett.*, vol. 49, pp. 128–130, 1986.

[3] R. Olshansky, W. Powazinik, P. Hill, V. Lanzisera, and R. B. Lauer, "InGaAsP buried heterostructure laser with 22 GHz bandwidth and high modulation efficiency," *Electron. Lett*, vol. 23, pp. 239–241, 1987.

[4] J. E. Bowers, B. R. Hemenway, A. H. Gnauck, and D. P. Wilt, "High speed InGaAsP constricted-mesa lasers," *IEEE J. Quantum Electron.*, vol. QE-22, pp. 833–844, 1986.

[5] K. Uomi, H. Nakano, and N. Chinone, "Ultrahigh-speed 1.55 μm $\lambda/4$-shifted DFB PIQ-BH lasers with bandwidth of 17 GHz," *Electron. Lett.*, vol. 25, pp. 668–669, 1989.

[6] C. A. Burrus, J. E. Bowers, and R. S. Tucker, "Improved very high speed packaged InGaAs PIN punch-through photodiode," *Electron. Lett.*, vol. 21, pp. 262–263, 1985.

[7] W. Stephens and T. Joseph, "A 1.3 μm microwave fiber optic link using direct-modulated laser transmitter," *J. Lightwave Technol.*, vol. LT-3, pp. 308–315, 1985.

[8] N. V. Jespersen and P. R. Herczfeld, "A comparison of optical distribution and steering mechanisms for phased array antennas," in *A/P Conf. Proc.* (Syracuse, NY), 1988, pp. 48–51.

[9] I. Koffman, A. S. Daryoush, and P. Herczfeld, "A fiber optic recirculating memory loop for radar and ECM applications," *Microwave and Opt. Technol. Lett.*, vol. 1, p. 81, 1988.

[10] W. Way, R. S. Wolff, and M. Krain, "A 1.3 μm 35 km fiber optic microwave multicarrier transmission system for satellite earth stations," *J. Lightwave Technol.*, vol. LT-5, pp. 1325–1332, 1987.

[11] T. E. Darcie, M. E. Dixon, B. L. Kaspar, and C. A. Burrus, "Lightwave system using microwave subcarrier multiplexing," *Electron. Lett.*, vol. 22, pp. 774–775, 1986.

[12] R. Olshansky and E. Eichen, "Microwave-multiplexed wideband lightwave systems using optical amplifiers for subscriber distribution," *Electron. Lett.*, vol. 24, p. 922, 1988.

[13] J. L. Gimlett, "Ultra high speed optical receivers," in *Proc. OFC '89* (Houston, TX), 1989, paper WJ1.

[14] L. W. Ulbricht and J. Schlafer, "A high-frequency laser package for microwave optical communications," *Proc. SPIE*, vol. 716, pp. 126–130, 1986.

[15] J. Schlafer and L. W. Ulbricht, "Packaging techniques for broadband microwave optoelectronic components," *Proc. SPIE*, vol. 995, pp. 48–52, 1988.

[16] W. Powazinik, R. Olshansky, E. Meland, and R. B. Lauer, "Semiconductor lightsources fabricated by vapor phase epitaxial regrowth," *Proc. SPIE*, vol. 723, pp. 94–99, 1986.

[17] J. Schlafer and M. Teare, "Photodetector design and packaging for optimum digital and microwave receiver performance," *Proc. SPIE*, vol. 722, pp. 217–221, 1986.

[18] E. Eichen and A. Silletti, "Bandwidth measurements of ultrahigh-frequency optical detectors using the interferometric FM sideband technique," *J. Lightwave Technol.*, vol. LT-5, pp. 1377–1381, 1987.

[19] J. Schlafer, C. B. Su, W. Powazinik, and R. B. Lauer, "20 GHz bandwidth InGaAs photodetector for long wavelength microwave optical links," *Electron. Lett.*, vol. 21, pp. 469–471, 1985.

[20] H. P. Hsu *et al.*, "Fiber optic links for microwave signal transmission," *Proc. SPIE*, vol. 716, pp. 690–695, 1986.

John Schlafer (M'65) received the B.S.E.E. degree from Rensselaer Polytechnic Institute in 1961 and the M.S.E.E. degree from the Polytechnic Institute of Brooklyn in 1963.

He became a Member of the Technical Staff in the Optical Communications Group at GTE Laboratories in 1963 and was initially involved in the development of techniques for microwave modulation and deflection of light. Subsequent research has included work on multiple wavelength optical modulators for laser film recording and projection displays, high-resolution laser scanners for optical radar, and laser-based stencil printers for shadow mask color CRT phosphor lithography. He has been most recently engaged in the design and characterization of optoelectronic components for fiber communication systems.

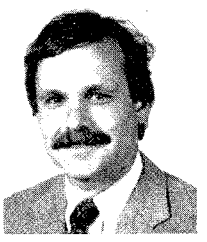

Robert B. Lauer (M'86) was born in York, PA, on March 9, 1942. He received the A.B. degree in physics from Franklin and Marshall College, Lancaster, PA, in 1964 and the M.S. and Ph.D. degrees in physics in 1966 and 1970, respectively, from the University of Delaware, Newark.

In 1970, he joined Itek Corporation's Central Research Laboratory in Lexington, MA, where he served as a Senior Scientist investigating the properties of oxide photoconductors. In 1974, he joined GTE Laboratories in Waltham, MA,

where his initial responsibilities included the growth, fabrication, and characterization of semiconductor light sources. Dr. Lauer was appointed Manager of the Optoelectronic Devices and Materials Department in 1981. His department has recently developed very wide bandwidth lasers and photodetectors for use in baseband digital, microwave, and subcarrier multiplexed fiber optic systems. The department also explored the feasibility of using high radiance LED's in single-mode fiber-optic systems. Current research is in the area of quantum well and strained quantum well lasers, semiconductor optical amplifiers, modulators, photodetectors, and photonic integrated circuits. Epitaxial capabilities include MBE, GSMBE, MOVPE, LPE, and halide VPE.

Dr. Lauer has received the Leslie H. Warner Award—GTE's highest technical award—for his contributions to semiconductor laser development. He has also received two GTE Technical Achievement awards. Dr. Lauer has contributed more than 50 papers to the technical literature in the area of semiconductor devices and materials, and he has filed several patents in this area. He is a member of OSA and Sigma Xi.